Potentiometric Response of Ag/AgCl Chloride Sensors in Model Alkaline Medium

Pargar, Farhad; Kolev, H; Koleva, Dessi; van Breugel, Klaas

DOI
10.1155/2018/8135492

Publication date
2018

Document Version
Final published version

Published in
Advances in Materials Science and Engineering

Hindawi
Advances in Materials Science and Engineering
Volume 2018, Article ID 8135492, 12 pages
https://doi.org/10.1155/2018/8135492

Research Article

Potentiometric Response of Ag/AgCl Chloride Sensors in Model Alkaline Medium

Farhad Pargar,[1] **Hristo Kolev**,[2] **Dessi A. Koleva**,[1] **and Klaas van Breugel**[1]

[1]*Department of Materials and Environment, Faculty of Civil Engineering and Geosciences, Delft University of Technology, Stevinweg 1, 2628 CN Delft, Netherlands*
[2]*Institute of Catalysis, Bulgarian Academy of Sciences, Acad. G. Bonchev Str., Bl. 11, 1113 Sofia, Bulgaria*

Correspondence should be addressed to Farhad Pargar; f.pargar@tudelft.nl

Received 30 January 2018; Revised 26 April 2018; Accepted 14 May 2018; Published 28 June 2018

Academic Editor: Luca De Stefano

The stability and reproducibility of an Ag/AgCl sensors' response in an alkaline medium are important for the application of these sensors in cementitious materials. The sensors' response, or their open circuit potential (OCP), reflects a dynamic equilibrium at the sensor/environment interface. The OCP response in an alkaline medium is affected by the presence of hydroxide ions. The interference of hydroxide ions leads to inaccuracies or a delay in the sensors' response to a certain chloride content. In this article, the potentiometric response (or OCP evolution) of the chloride sensors is measured in model solutions, resembling the concrete pore water. The scatter of the sensors' OCP is discussed with respect to the interference of hydroxide ions at varying chloride concentration in the medium. The deviation of the sensor's response from its ideal performance (determined by the Nernst law) is attributed to dechlorination of the AgCl layer and the formation of Ag_2O on the sensor's surface. Results from the surface XPS analysis of the AgCl layer before and after treatment in alkaline medium confirm these observations in view of chemical transformation of AgCl to Ag_2O.

1. Introduction

Ag/AgCl electrodes have been used as "chloride sensors" in cementitious materials for nondestructive and continuous monitoring of the free chloride concentration [1–3]. The stability and reproducibility of the sensors' response in alkaline medium, for example, cementitious materials, were not sufficiently addressed [4–7]. For instance, the observed difference between the responses of identically prepared chloride sensors in an environment with a predefined chloride content is still a subject of discussion. Therefore, the performance of Ag/AgCl electrodes in alkaline medium needs further investigation.

The open-circuit potential (OCP) of the chloride sensor, similar to the electrode potential of any metal in its adjacent environment, can be measured versus a known reference electrode. For an Ag/AgCl sensor, the OCP reflects the chloride content in the medium following (1) or the Nernst equation:

$$E_{\mathrm{Ag/AgCl}} = E^{0}_{\mathrm{Ag/AgCl}} - 2.303\frac{RT}{nF}\lg[a_{\mathrm{Cl^-}}], \quad (1)$$

where $E_{\mathrm{Ag/AgCl}}$ is the measured OCP of the sensor, $E^{0}_{\mathrm{Ag/AgCl}}$ is the standard electrode potential for the Ag/AgCl electrode (V), $a_{\mathrm{Cl^-}}$ is the activity of the chloride ions (mol·dm^{-3}) in the vicinity of the electrode, R is the gas constant (J·mol^{-1}·K^{-1}), F is the Faraday constant (C·mol^{-1}), and T is the absolute temperature (K). The above equation shows the linear relationship between the OCP of the sensor (i.e., $E_{\mathrm{Ag/AgCl}}$) and the logarithm of the chloride ions activity ($a_{\mathrm{Cl^-}}$) in a solution. In other words, a certain equilibrium potential (or the measured OCP) at the Ag/AgCl interface reflects the chloride ions activity and hence the chloride ions concentration in the medium. The chloride concentration is derived from the chloride ion activity using the activity coefficient (γ) [8–10]:

$$a_{\mathrm{Cl^-}} = C_{\mathrm{Cl^-}} \cdot \gamma_{\mathrm{Cl^-}}. \quad (2)$$

In an alkaline medium, as the pore water in cementitious materials, with zero or low chloride content, the measured

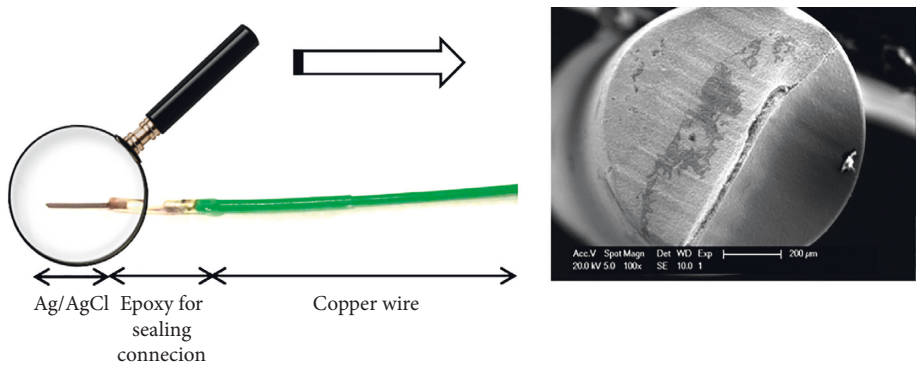

Figure 1: The as-produced Ag/AgCl chloride sensor.

OCP response of a sensor would deviate from the one according to the Nernst equation for an Ag/AgCl interface. The interference of hydroxide ions would determine an OCP response, not proportional to the activity of chloride ions only. Hence, the sensor's OCP is associated with the ratio of chloride to hydroxide ions at the sensor's surface [6, 9–14]. In such cases, the measured OCP does not only present the Ag/AgCl equilibrium (3) but also reflects a mixed potential described by the $Ag/AgCl/Ag_2O$ equilibrium (4).

$$Ag + Cl^- \leftrightarrow AgCl + e^- \quad (3)$$

$$2AgCl + 2OH^- \leftrightarrow Ag_2O + 2Cl^- + H_2O \quad (4)$$

Consequently, with the gradual transformation of silver chloride to silver oxide, the OCP response of the sensor is no longer proportional to the activity of chloride ions in the medium; hence, the stability and reliability of the sensor's measurement are largely affected and/or limited. This subject is not sufficiently addressed in the current state of the art, although it is of significant importance for the practical application of a chloride sensor of this type.

Additionally, the physical properties of the AgCl layer would determine the interaction of sensor/medium and the OCP response of the sensors, respectively [15–18]. The surface properties (morphology and microstructure) of the AgCl layer will affect the surface chemistry of the sensors. The level of surface chemistry alterations was found to be directly linked to the thickness, morphology, and microstructure of the AgCl layer, which were dependent on the anodization regime used for the sensor preparation [19–22]. For instance, chemical recombination and/or the presence of oxygen or carbon-based impurities on the sensors' surface would be responsible for a deviation of the sensors' response from the one expected for a purely Ag/AgCl interface [17]. Therefore, the surface properties of an AgCl layer would also be important for the stability of the sensor's response, when in contact with a chloride-free or a chloride-containing alkaline medium.

This paper presents the OCP evolution of Ag/AgCl sensors in a model alkaline environment. Sensitivity, stability, and reproducibility of the chloride sensors in different solutions were assessed. Calibration of the sensor was performed and compared to the available literature data. The potentiometric response of the sensors was recorded in conditions when the chloride concentration in the aqueous medium was either constant or varying. Hence, the reversibility of the sensors was also evaluated. The paper concludes with the experimental evidence for the chemical transformation of the AgCl layer in contact with an alkaline medium and also defines the chloride ions' detection limits in such a medium.

2. Experimental Materials and Methods

2.1. Ag/AgCl Sensors. The Ag wires of 99.5% purity, 1 mm diameter, were supplied by the Salomon's Metalen B.V., Netherlands. The Ag wires were cleaned for two hours in concentrated ammonia and then immersed in deionized water overnight, prior to anodization in 0.1 M HCl solution (pH ~ 1.4). The anodization was carried out in a conventional three-electrode cell arrangement, where the Ag wire (1 cm length) was the working electrode, a Pt mesh was the counterelectrode, and a saturated calomel electrode (SCE) was the reference electrode. The Ag wires were anodized for an equal duration of 1 h but at two different current densities. The designed codes for sensors were based on the anodization regime used for sensor preparation, that is, 0.5 mA/cm^2 (sensor A) and 4 mA/cm^2 (sensor D). The different anodization regimes resulted in a different thickness of the AgCl layer, forming on the Ag substrate, that is, ~10 μm for sensor A and ~40 μm for sensor D. The anodized Ag wires (i.e., the sensors as produced) were soldered to a copper wire, and the junction was protected with an epoxy resin (Figure 1). The final exposed length of the sensors was 1 cm. The sensors were stored out of direct sunlight until the moment of testing.

2.2. Microscopy and X-Ray Analysis. For microscopic observation of the Ag/AgCl interface, the Ag wires were narrowed prior to anodization. The narrowed section was stretched from two sides to obtain the cross section resembling a fracture surface. The surface morphology and cross section of the AgCl layers were analyzed using environmental scanning electron microscopy, Philips-XL30. The samples were examined under an accelerating voltage of 20 kV in high vacuum mode.

XPS analysis was performed on Ag foil with a surface area of 2.4 cm^2 per sample (1 cm width, 2 cm length, and 0.005 cm thickness). The Ag foils were anodized for one hour at 0.5 mA/cm^2 in 0.1 M HCl solution, that is, conditions

Table 1: Solutions for calibration of the chloride sensors.

Number	Solution	pH	Chloride concentration (mM)
1	Deionized water	6	1, 2, 4, 8, 16, 31, 64, 125, 250, 500, 1000
2	Cement extract solution*	12.8	12, 14, 16, 20, 27, 44, 77, 142, 260, 513, 1008
3	Simulated pore solution	13.6	1, 2, 4, 8, 16, 31, 64, 125, 250, 500, 1000

*Cement extract solution contains 12 mM chloride content due to the mixing water and chloride at levels of <0.03% in the original cement (ENCI, NL specifications).

Table 2: Model solutions and criteria for sensors' performance.

Test series	Used medium	pH	Chloride concentration (mM)	Purpose of OCP measurement in this environment (criteria for sensors' performance)
1	Simulated pore solution (SPS)	13.6	0	*Stability*: OCP variation in chloride-free alkaline solution (Figure 2)
2	Cement extract solution (CE)	12.8	20, 260	*Reproducibility*: dependent on different properties of the AgCl layer (Figure 4)
3	Simulated pore solution (SPS)	7, 9, 12.8, 13.6	1, 2, 4, 16, 62, 250	*Reliability*: interference of hydroxide ions and chloride detection limits (Figure 6)
4	Cement extract solution (CE)	12.8	12, 14, 16, 20, 27, 44, 77, 142, 260, 513, 1008	*Reversibility*: response to continuous addition of chloride (Figures 7 and 8)
5	Simulated pore solution (SPS)	13.6	0, 125, 1000	

identical to those used for the production of sensor A. The flat Ag/AgCl sensor was immersed in chloride-free NaOH solution (pH = 13.7), and the sensor's OCP was measured continuously, reaching a stable value around 100 mV after 8 days of treatment. The surface composition of the "treated" sensor was determined by XPS, and the results were compared to those of identically produced, nontreated sensor. The XPS measurements were carried out in an AXIS Supra electron spectrometer (Kratos Analytical, Ltd.) using monochromatic AlKa radiation with photon energy of 1486.6 eV. The samples were mounted with metal clips on the sample holder. The samples and the sample holder were grounded, and a neutralizer was used to compensate the charge on the surface. The high-resolution scans have been recorded with 20 eV pass energy. The energy calibration was performed by referencing the carbon (C1s) line of adsorbed adventitious hydrocarbons to 285.0 eV. The binding energies (BE) were determined with an accuracy of ±0.1 eV. Processing of the measured spectra includes a subtraction of Shirley-type background [23].

2.3. Model Media. Different model solutions used in this work were as follows: deionized water (DW) of pH ~ 6; simulated concrete pore solution (SPS) (0.05 M NaOH + 0.63 M KOH + sat. $Ca(OH)_2$) of pH ~ 13.6 and cement extract (CE). The cement extract (CE), of pH ca. 12.8, was obtained by mixing cement powder (CEM I 42.5 N) and tap water at the ratio of 1:1. The bottled mixture was rotated for 24 hours, followed by filtration for obtaining the extract. The model solutions were chloride free or chloride contaminated, using NaCl additions.

Tables 1 and 2 present all model solutions and their composition. To be noted is that the response of sensors A and D was recorded in chloride-free and chloride-containing alkaline medium (CE), while calibration and evaluation for reproducibility, reliability, and reversibility were tested for sensor A only. This was based on the decision made for sensor A as the better choice for sensor's application in alkaline medium and after considering various points, including surface morphology, composition, potential constraints towards ion transport, and electrochemical state in an aqueous medium for sensor A, compared to sensor D.

2.4. Open-Circuit Potential (OCP) Measurements. The records of OCP versus time were used to evaluate the sensor's performance in different solutions (Tables 1 and 2). The motivation behind OCP measurement in each environment and test series are listed in Table 2, reflecting the evaluation criteria. The setup used to perform these potentiometric measurements comprised a chloride sensor (working electrode) and a reference electrode (SCE), using a PGSTAT 302N potentiostat (Metrohm Autolab B.V., the Netherlands). In this study, the reference electrode was in contact with the solution only for a few seconds during OCP records. Hence, the use of a double junction electrode was not found to be necessary.

3. Results and Discussion

3.1. Sensors' Response (OCP) in Alkaline Solutions. The sensors' OCP shifts in cathodic direction with increasing chloride concentration in the medium (in accordance with (1) and (3)). For instance, the OCP response of a chloride sensor in 250 mM and 500 mM chloride contents is 6 mV and 23 mV versus SCE, respectively [14]. In a chloride-free environment, the sensors' OCP reflects a mixed potential described by a dynamic exchange equilibrium, similar to (4). In this condition, the OCP values are expected to be more anodic (ca. 100 mV to 150 mV versus SCE [14, 24, 25]), due to

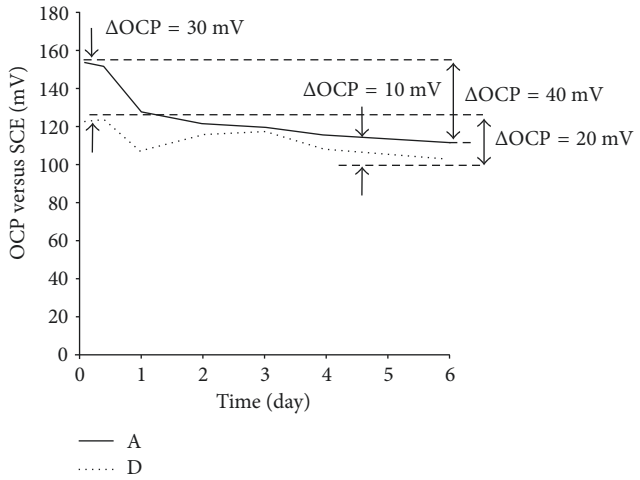

Figure 2: Evolution of OCP values of the sensors A and D in chloride-free simulated pore solution (SPS).

a mixed potential, arising from OH^- ions interference [5]. The level of OH^- ions interference depends on the chloride ion concentration (i.e., the OH^-/Cl^- ratio). In this regard, a chloride detection limit of 10 mM chloride content was reported [5].

The OCP of sensors A and D in chloride-free simulated pore solution (SPS) is depicted in Figure 2. The response of identical (replicate) sensors in cement extract (CE), containing 20 mM and 260 mM chloride concentration, is depicted in Figures 4(a) and 4(b).

3.1.1. Chloride-Free Alkaline Medium. The OCP response of sensors A and D was monitored during 6 days of immersion in chloride-free simulated pore solution (Figure 2). The initial OCP value for sensor A (ca. 150 mV) was more anodic than that for sensor D (ca. 120 mV). The sensors' OCP gradually shifted to cathodic potentials, and after 6 days of immersion, it reached to 112 mV for sensor A and 102 mV for sensor D. In other words, the difference between the OCP response of sensors A and D decreased from 30 mV in the first hours of immersion to 10 mV after 6 days (Figure 2). The OCP variation in time and establishment of a stable OCP value is not only dependent on the sensor type but is also due to AgCl dechlorination and Ag_2O formation at the sensor's surface, as previously introduced. The observed performance of the sensors is governed by an exchange equilibrium, where the expected continuous transformation of AgCl to silver oxide changes the activity of silver ions (Ag^+) near the silver substrate. As a result, a mixed potential develops at the sensors' surface [14, 26], shifting the OCP from around 150 mV towards 99 mV (versus SCE) [25, 27, 28]. The difference between the initial OCP value and that established after 6 days is wider for sensor A (40 mV) than for sensor D (20 mV). Because the OCP alteration would be a result of dechlorination of the AgCl layer (AgCl to Ag_2O transformation), the wider OCP range from the initial to the stabilized OCP value for sensor A (40 mV) most probably reflects a higher amount of purely AgCl at the surface of this sensor.

This observation can be explained by the different morphology and microstructure of the AgCl layer for sensors A and D. The AgCl layer on the Ag substrate of sensors A and D is shown in Figure 3. The increase in the current density from 0.5 mA/cm^2 (sensor A) to 4 mA/cm^2 (sensor D) resulted in thicker AgCl layer, variation in morphological features, and appearance of additional inner layer with smaller AgCl grains close to the Ag substrate (Figure 3(b)). A heterogeneous and less adherent AgCl layer (as in sensor D) would lead to an immediate and enhanced oxidation at the Ag/AgCl interface when it is in contact with external alkaline medium, that is, dissolution of AgCl [17]. This explains the smaller difference between the initial, more cathodic OCP response for sensor D (ca. 120 mV) and that established at the end of the test (ca. 100 mV). A high-current density would also increase the impurities, such as metallic silver (Ag^0) together with the oxygen and carbon-based compounds in the AgCl layer [22]. More details on microscopic and surface analysis of the AgCl layer of the sensors after anodization at various current densities can be found in [22, 29].

The properties of the AgCl layer not only affect the sensor's response in chloride-free alkaline medium (as above shown) but also would determine the sensor's response in chloride-containing alkaline medium. This is the subject of discussion in the next section.

3.1.2. Sensors' Reliability and Reproducibility versus Structure of the AgCl Layer. The reliability and reproducibility of the sensor's response in chloride-containing medium can be affected by the AgCl layer properties. Reproducibility of the sensor's response is specifically important in view of the sensor's performance in alkaline medium [30, 31]. In the following, the reproducibility of the OCP response of replicates of sensors A and D in CE with 20 mM and 260 mM chloride content is addressed.

The OCP response of three replicates of sensor A (A1, A2, A3) and sensor D (D1, D2, D3) (Figure 4) was monitored for 2200 s. The OCP response of sensors D varied significantly throughout the test, if compared to the relatively stable response of sensors A (Figure 4). In less than a 100 s, sensors A reached to the stable values of 85 ± 1.5 mV and 25 ± 0.2 mV in CE of 20 mM and 260 mM chloride concentrations, respectively. In contrast, a relatively stable OCP for the D sensors was observed after 1800 s with a value of 78 ± 3 mV for CE with 20 mM chloride concentration and 23 ± 2 mV for CE with 260 mM chloride concentration. The OCP response of sensors A was reproducible. This is evident from the lower standard deviation of the OCP response of sensors A (0.2–1.5 mV) in comparison to that of sensors D (2-3 mV). The lower reproducibility for sensors D can be attributed to the heterogeneity and multilayered structure of the AgCl layer for these sensors (discussed in Section 3.1.1).

Additionally, the following observation is important to be specifically addressed: in the initial period, the higher instability of sensors D, compared to sensors A, was obvious (Figure 4 records prior to 1200 s). This means that sensors D initially "underestimated" or "overestimated" the chloride content, while sensors A present an almost immediate

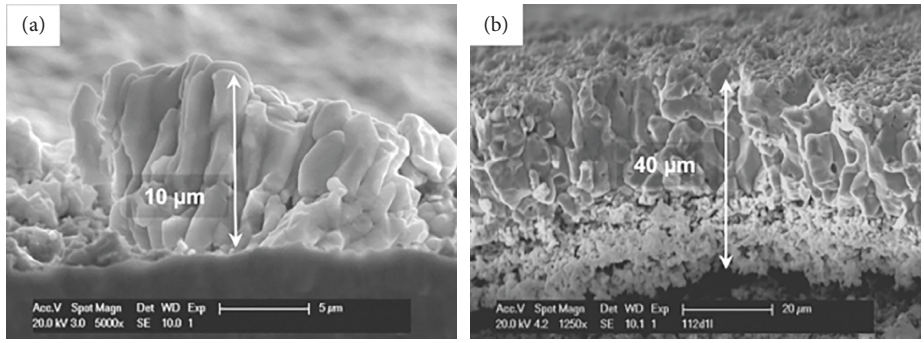

Figure 3: Micrographs of an AgCl layer, deposited at different current densities: (a) cross section of sensor A at 0.5 mA/cm^2; (b) cross section of sensor D at 4 mA/cm^2.

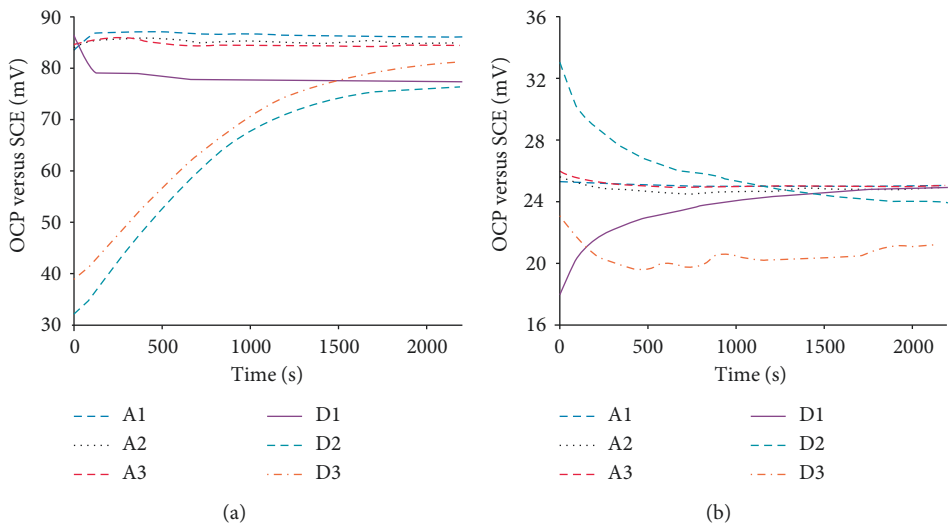

Figure 4: OCP response of replicates of sensors A and D in chloride-containing cement extract (CE): (a) 20 mM chloride content; (b) 260 mM chloride content.

accurate response. The different microstructural properties of the Ag/AgCl interface for A versus D sensors (Section 3.1.1) are supposed to be responsible for the differences in the OCP response. Except the already discussed considerations, the limitation of ion transport of any kind at the sensor/medium interface or limitation of electron transport along the sensors' conductive surface will also be reflected in variation in the time to establish an equilibrium condition.

Consequently, when the sensors are in contact with the chloride-containing alkaline medium, the chloride ions diffusing into the AgCl layer will alter the Ag^+ activity so that a new equilibrium is established on the sensors' surface (3). A fast equilibrium is achieved in a short period for sensor A, reflected by a stable OCP in the solutions (Figure 4). In the presence of impurities, such as Ag^0, a lower concentration of Ag^+ will be available at the surface of the Ag substrate. A lower concentration of Ag^+ would subsequently shift the sensor's OCP towards more negative (cathodic) potentials [32] or determine an erratic response and instability (Figure 4). Therefore, a longer time is needed for establishing an equilibrium condition at the Ag/AgCl interface of the sensors with a thicker and more heterogeneous AgCl layer, as in sensor D, compared to sensor A (Figure 4). For all further tests and investigations in this work, sensor A was chosen to proceed with. This is because the OCP response of sensor A is less affected by the surface transformations due to the anodization regime itself (e.g., heterogeneity of the AgCl layer); hence, a better performance of the sensor is as expected.

3.2. Sensor's Calibration. Calibration of an Ag/AgCl sensor is a necessary step in evaluating its performance, when in contact with the external medium. The calibration curve for the chloride sensor is, essentially, the link of the sensor's OCP to the activity of chloride ions in a solution. For this purpose, the OCP of the Ag/AgCl sensor was recorded in deionized water (DW), simulated pore solution (SPS), and cement extract (CE) of varying chloride content, or in the so-called "calibration" solutions (Table 1). The chloride activity was calculated from the chloride concentration by using the activity coefficient (2). The mean activity coefficient for NaCl solution in a standard condition was derived from the literature [8, 28]. Figure 5 presents the recorded responses, together with values reported by other researchers for identical or similar conditions.

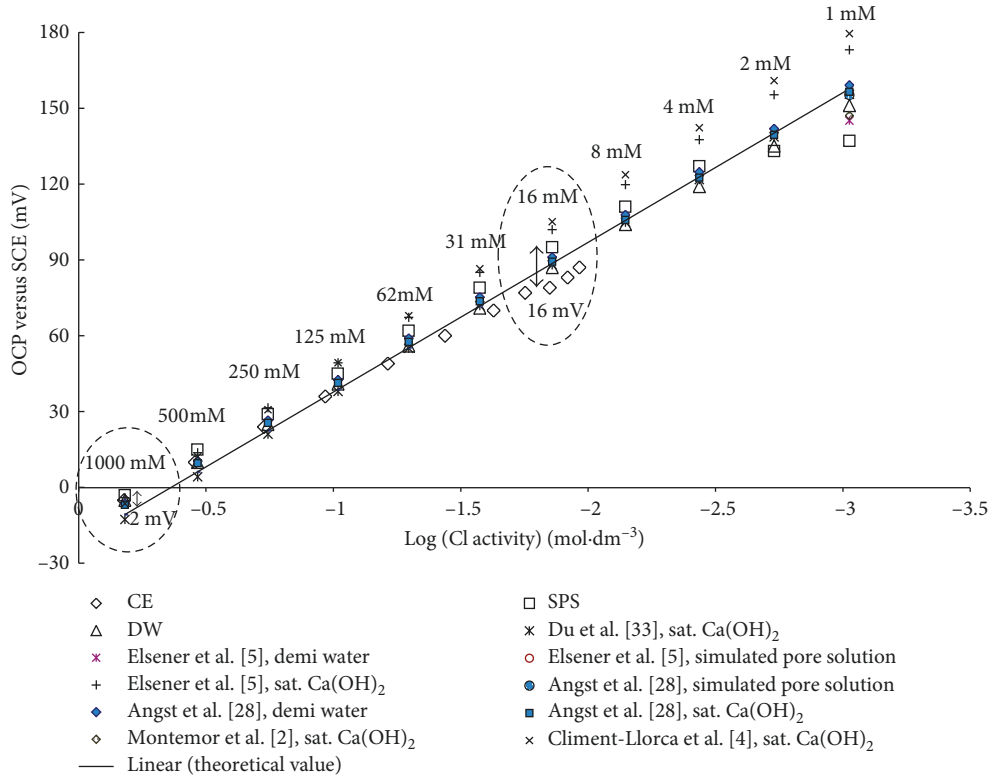

Figure 5: OCP response of chloride sensors versus the activity of chloride ions in different solutions.

Linear regression was employed to derive the coefficient of determination (R^2). In DW, the interference of hydroxide ions was negligible. Therefore, the sensor in DW responded accurately to a wide range of chloride concentration (from 2 mM to 1000 mM with an accuracy of $R^2 = 0.999$). In the same range of chloride concentration, but in the SPS medium, R^2 equals to 0.985. For increasing the degree of linearity to $R^2 = 0.999$, the chloride detection limit in SPS should be 8 mM. This value is similar to the reported 10 mM detection limit for an Ag/AgCl sensor in alkaline medium (pH 13.7) [14, 28]. Therefore, the linear regression for the results in SPS was performed for chloride concentration higher than 8 mM. The following equation was applied for the regression analysis:

$$E\,(\text{mV versus SCE}) = m_0 + m_1 \cdot \lg a_{\text{Cl}}. \quad (5)$$

Table 3 summarizes the results of linear regression for all solutions. The slope of the calibration curves varies from −50 mV to −62 mV with an average of −56 mV. Although a good agreement is observed between the results (slope) recorded in this study and the values reported in the literature (Table 3), the experimental and theoretical slopes following the Nernst equation are in fact different, that is, −50 mV versus −59 mV, respectively. This deviation from the theoretical value (i.e., from ideal performance) can be related to the chloride ions' activity coefficient. While the theoretical Nernst slope is based on thermodynamic equilibrium and spontaneity of the reactions at the sensor's surface in standard conditions, the experimental Nernst slope is derived in the conditions of the relevant experiments. Changes in the test medium, such as varying alkalinity or ionic strength, resulted in calibration curves with different slopes (Table 3). Hence, the difference between theoretically and experimentally derived slopes of the calibration curves is logic and as expected.

What can be also observed in Figure 5 is that irrespective of the medium and at low chloride concentration, the OCPs of the sensors vary in a wider range. This is valid for both the experimentally derived values and those reported by other researchers. For example, more than 40 mV difference in OCP was observed at 1 mM chloride concentration, while the OCP variation decreased to less than 10 mV at chloride concentration of 1000 mM. This is regardless of the alkalinity and ionic strength of the solution. In this work, the difference amongst the sensor's OCP in DW, CE, and SPS was 16 mV at 16 mM chloride concentration, decreasing to 2 mV at 1000 mM chloride concentration. The larger scatter at lower chloride content is due to the interference of hydroxide ions, resulting in a limited accuracy of the sensor in determination of the chloride concentration. Because the hydroxide ions interference would be larger in solutions of higher pH, a chloride content detection limit is determined in view of the practical application of Ag/AgCl sensors in the alkaline medium as concrete. This point is discussed further in the next section.

3.3. Interference and Detection Limits. As already pointed out, the performance of chloride sensors in alkaline medium is affected by a chloride detection limit. Below this detection limit, the sensors respond inaccurately to the chloride content [9, 10]. The reason for the existence of such a limit

Table 3: Slope of the calibration curves and results from the statistical analysis in simulated pore solution (SPS), cement extract solution (CE), and deionized water (DW).

Solution	This work			Slope from other studies				
	Slope (m_1 in (5))	Axis (m_0 in (5))	R^2	[28]	[5]	[2]	[4]	[33]
CE	−49.73	−12.48	0.998	—	—	—	—	—
SPS	−58.11	−13.31	0.999	−57.8	−54	—	—	—
DW	−55.39	−15.69	0.999	−58.3	−50	—	—	—
Sat. $Ca(OH)_2$	—	—	—	−57.6	−59	−53.46	−61.72	−56.02
Theoretical value	−59.16	−21.4	1					

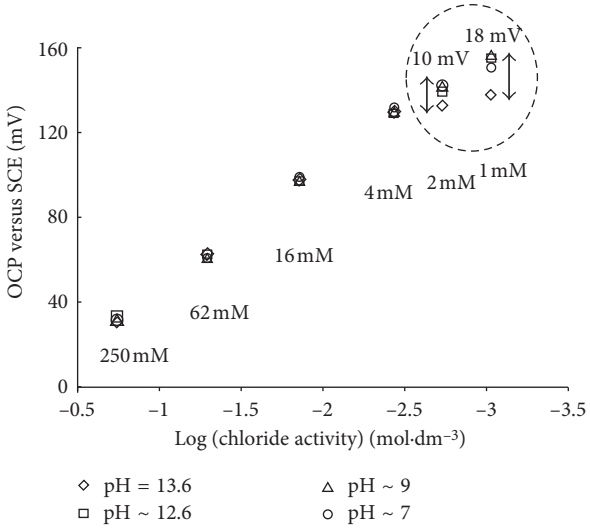

Figure 6: The effect of pH on the OCP response of the chloride sensor.

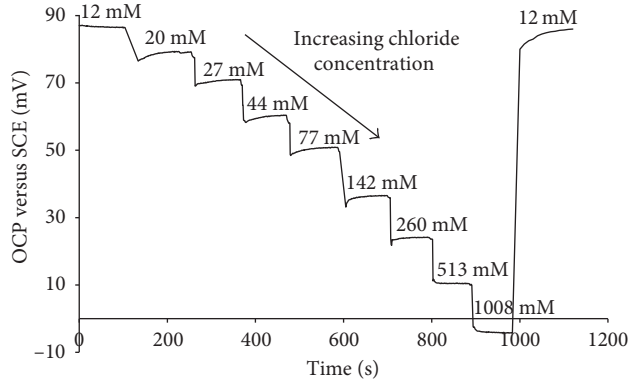

Figure 7: Chloride sensor's response in cement extract solution (CE) at continuously changed chloride concentration.

and imprecise sensors' response is the interference of hydroxide ions, which are readily available in the solution. A chloride detection limit of around 10 mM was reported in previous works [12, 14, 28]. To further investigate this, the OCP of the chloride sensors was measured in simulated pore solutions of different pH (7.0, 9.0, 12.6, and 13.6) and varying chloride concentration (1 mM, 2 mM, 4 mM, 16 mM, 62 mM, and 250 mM) (Figure 6 and Table 2—test series 3). The pH of the solutions was modified by a dropwise addition of concentrated nitric acid. The OCP in each solution was recorded for 600 s, a sufficient time interval for achieving a stable response, including reflection on the contribution of hydroxide ions' interference.

As can be observed in Figure 6, the sensor's OCP shifts to a more cathodic value when the alkalinity of the solution increases from neutral to pH 9 and pH 13.6. This OCP drift reflects the hydroxide ions interference and is more pronounced at low chloride concentration, that is, 1 mM and 2 mM (circled region in Figure 6). The observation is in line with the previously discussed results in Figure 5 for the same chloride content but for varying chemical composition and ionic strength of the external medium.

The difference amongst the sensor's OCP in solutions containing 1 mM and 2 mM chloride concentrations is 18 mV and 10 mV, respectively. These OCP differences narrow down to 1-2 mV upon increasing the chloride content to 4 mM. A difference of 1 to 2 mV in OCP values can be considered as negligible [34]. Consequently, the chloride sensors can be used for a relatively accurate determination of the chloride content in alkaline solutions, where the chloride concentration is higher than 4 mM. The reasons behind the higher or lower levels of hydroxide ions interference to the sensors' response in alkaline medium are linked to the transformation of silver chloride to silver oxides on the sensor's surface. This transformation is governed by both the pH and ionic strength of the medium, in addition to the actual chloride content. The transformation of silver chloride to silver oxides and its subsequent influence on the sensors' response will be confirmed by outcomes from surface XPS analysis of the AgCl layer, presented in Section 3.5.

3.4. Sensitivity and Reversibility of the Chloride Sensor. The sensitivity of the sensor is reflected by its expected OCP response to a predefined chloride content. The reversibility is the ability of the sensor to return the expected nernstian response upon changing the environment from chloride free to chloride containing and vice versa. The sensitivity was already discussed with relevance to the sensor's response in various solutions (Figure 4). The reversibility is discussed in this section in view of the sensors' response upon changing the medium from chloride free to chloride containing.

Both sensitivity and reversibility are illustrated in Figure 7. The figure shows the recorded OCP response of a sensor immersed in alkaline cement extract (CE) in which a continuous change of the chloride content was applied. By increasing the chloride concentration from 12 mM to 1008 mM, the OCP changes from anodic to cathodic values. The experimentally derived values are well in line with those derived from the

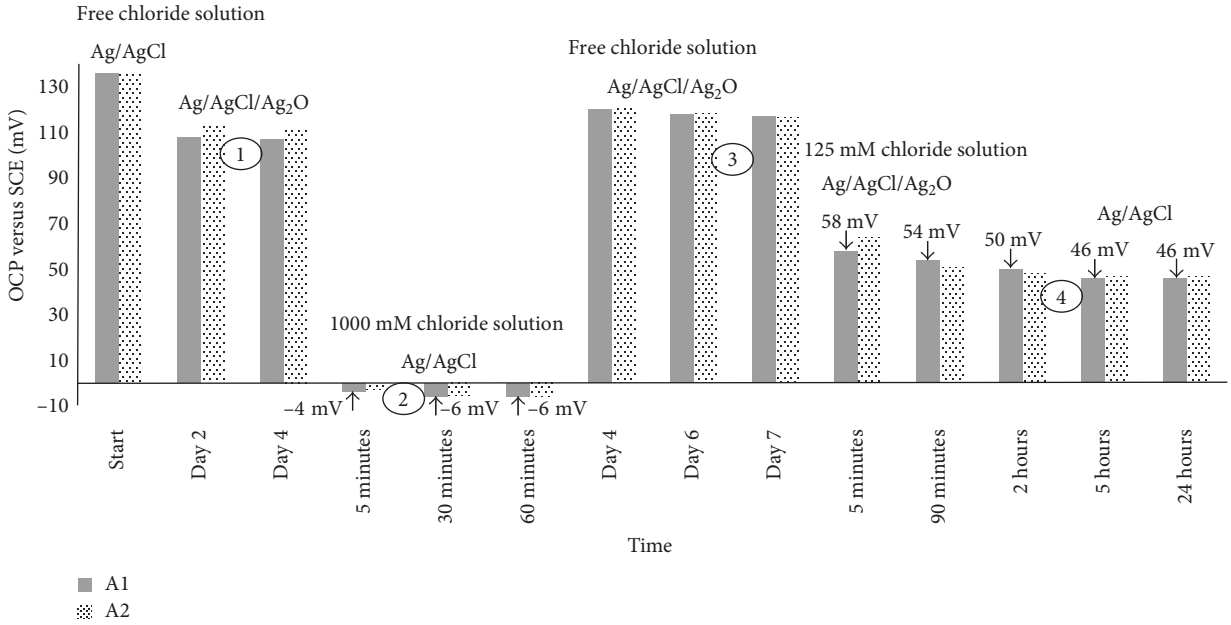

Figure 8: Sensor's response in chloride-free and chloride-containing simulated pore solution (SPS).

Nernst equation. For instance, at chloride content in the medium of 20 mM, 77 mM and 513 mM, the sensor's response should be 84 mV, 52 mV, and 6 mV, which are well in line with the recorded 79 mV, 50 mV, and 10 mV (Figure 7).

In the event of changing the chloride concentration from 1008 mM to 12 mM (i.e., a sharp decrease in chloride content), the sensor's OCP returns in approximately 60 s to the initial and expected Nernstian response of 87 mV. This observation demonstrates the good sensitivity and reversibility of the sensor, both of importance for the precision of chloride detection.

Reversibility is important in view of the Ag/AgCl sensor's application in cement-based materials. This has a high practical significance for chloride sensors embedded in chloride-free reinforced concrete. In these conditions, the sensor should remain "active" and accurately respond to altered chloride ions' concentration in the medium.

The reversibility of the sensor was tested in chloride-free and chloride-containing alkaline solution, SPS (Table 2—test series 5). In the absence of chloride ions, the transformation of AgCl to Ag_2O is a preferential reaction, in accordance with (4).

The resulting OCP in chloride-free simulated pore solution (SPS) will be anodic (more positive) and will stabilize around values, reflecting the equilibrium at an Ag/AgCl/Ag_2O interface. Upon addition and/or increase of chloride ions concentration, the OCP shifts to cathodic (more negative) values, reflecting the equilibrium at an Ag/AgCl interface. The rate at which these OCP changes occur, and/or are reversed, reflect the altered chloride content in the medium, as well as the level of the sensor's reversibility.

The above considerations are illustrated in Figure 8. The sensor (two replicates of sensor A, i.e., A1 and A2) was immersed in chloride-free SPS for four days, followed by addition of chloride at the level of 1000 mM. Next, the sensor was transferred to a fresh chloride-free SPS for three subsequent days, after which the chloride content was changed to the level of 125 mM in the solution. The OCP was recorded during all above steps, and the established values can be summarized in four main regions (Figure 8). In regions ① and ③, the OCP values were anodic, while in regions ② and ④, a cathodic shift was observed. Region ① presents the point of immersion of the sensors in chloride-free SPS and subsequent treatment, whereas after four days, the OCP stabilizes from the initial ca. 137 mV to around 110 mV. This change reflects the gradual transformation of silver chloride to silver oxide and the establishment of an equilibrium at the Ag/AgCl/Ag_2O interface.

Upon the addition of chlorides in region ② (adjusted to 1000 mM), the sensors react to the chloride ions content by an OCP shift to ca. −6 mV. This corresponds to a change of the Ag/AgCl/Ag_2O interface in the region ① to an Ag/AgCl interface, dominant for the region ②. The OCP stabilization in the region ② was achieved between 30 and 60 min.

In the next step, region ③, the chloride sensor was reimmersed in chloride-free SPS. In region ③, the initial OCP was ca. 120 mV, that is, more anodic than the final OCP measured in the region ① (110 mV) and in the direction of approaching the OCP of a sensor at the beginning of treatment (region ①, ca. 137 mV). This means that the sensor's surface partially recovers the originally present AgCl layer in conditions of sufficient chloride concentration in the medium (1000 mM in this case), by following a transformation of Ag_2O to AgCl. With prolonged treatment in the chloride-free conditions in the region ③, the established OCP at ca. 110 mV is again due to Ag_2O formation, similarly to what takes effect at the end of the region ①.

Upon the addition of chlorides in region ④, reaction mechanisms as in region ② were relevant. However, in region ④, the chloride concentration was adjusted to a lower level, that is, 125 mM. The OCP reached to values of 46 mV

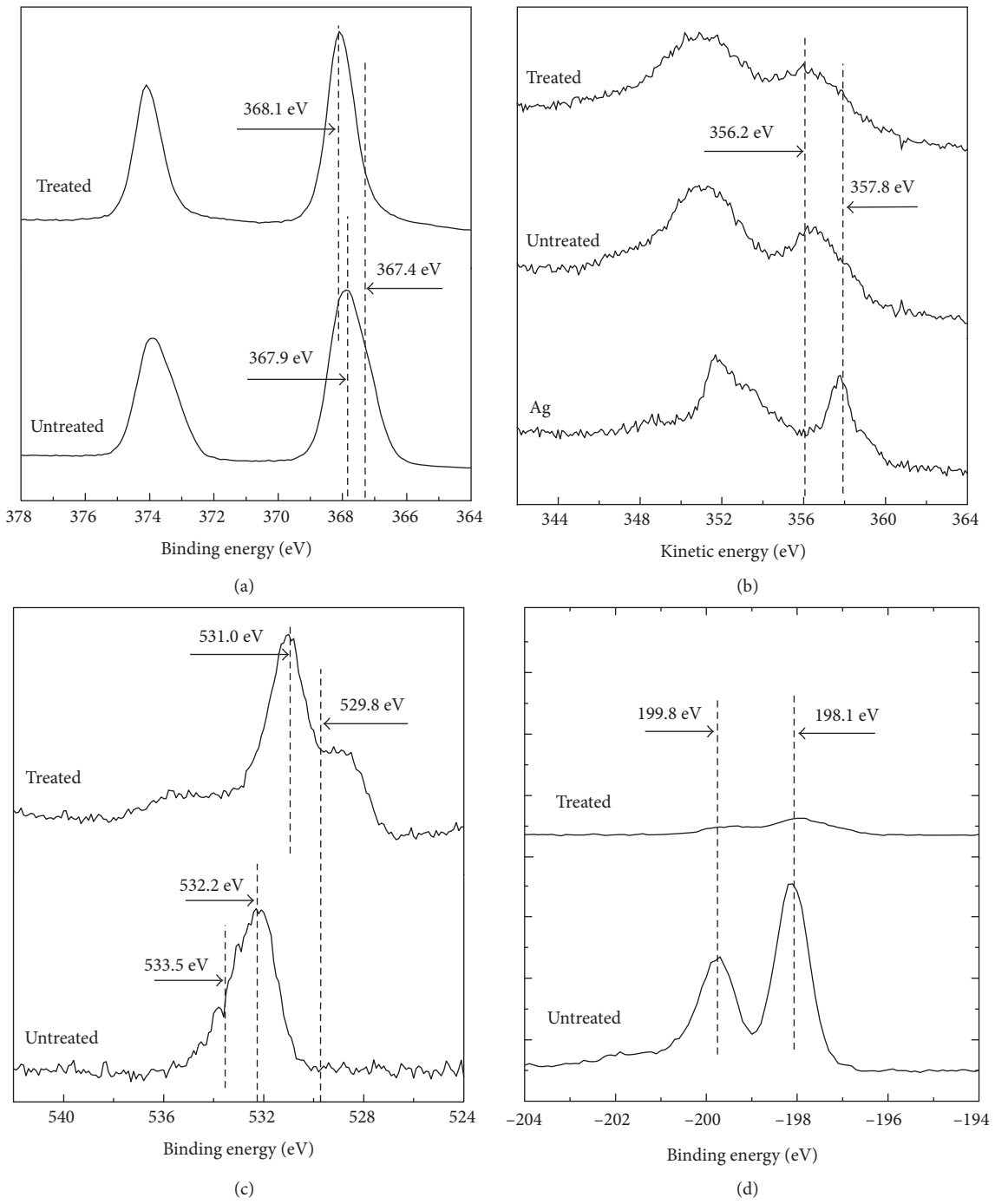

Figure 9: High-resolution surface XPS spectra before and after conditioning in NaOH solution: (a) Ag3d photoelectron lines; (b) AgMNN Auger lines; (c) O1s photoelectron lines; (d) Cl2p photoelectron lines.

and stabilization occurred within 5 h of treatment. If the time to establishment of a stable OCP in regions ② and ④ is to be assessed, clearly higher chloride content (region ②) triggers a faster stabilization (30 min) versus the 5 h, needed at lower chloride content (region ④). Therefore, the reversibility of the sensor is related to the transformation rate of Ag_2O to AgCl, which is dependent on the chloride concentration in the external medium.

As mentioned above, the transformation of AgCl to Ag_2O is responsible for the deviation of the sensor's response from the expected performance. In the following section, the AgCl to Ag_2O transformation is justified by analyzing the sensors' surface chemistry and surface composition of the AgCl layer before and after conditioning in alkaline medium.

3.5. Surface Composition of AgCl Layer before and after Treatment in SPS. The high-resolution spectra from the surface XPS analysis of sensor A are presented in Figure 9. The XPS analysis does not claim absolute values for chemical composition of the AgCl layers, but it provides an accurate

(quantitative) comparison of equally handled samples before and after conditioning in alkaline medium. The NIST XPS database was consulted [35] for the binding (BE) and kinetic energies (KE) for the elements.

After conditioning in NaOH solution, the Ag3$d_{5/2}$ peak at 368.1 eV (Figure 9(a)) cannot be assigned to a solely one compound [36–38]. The AgMNN peak for the treated sensor (Figure 9(b)) shows a pattern similar to the untreated sensor pattern, however, with a kinetic energy of 356.0 eV and a broader high-energy peak. This broadening is characteristic in situations, where Ag exists in a different state (e.g., Ag^0, AgOH, Ag_2O, and AgO). The modified Auger parameter (α') was also determined. The α' was defined as $\alpha' = \text{KE (A)} + \text{BE (P)}$, where KE (A) represents kinetic energy of the Auger electron (A) and BE (P) represents binding energy of the photoelectron (P). The α' with a value of 724.1 for both treated and untreated sensor can be equally attributed to AgO (724.2), Ag_2O (724.3), and AgCl (723.5) [36]. The O1s pattern (Figure 9(c)) for the treated sensor depicts a shift towards lower energies and a characteristic broadening, starting at 528 eV. This is a strong evidence for the transformation of AgCl to silver oxides due to conditioning in alkaline medium. Low-energy peaks or low-energy broadening in the O1s pattern indicate oxygen in metal oxides. Along with the significantly different O1s patterns for the sensor before and after the treatment (Figure 9(c)), the above features clearly show the presence and strong contribution of silver oxides on the sensor's surface after the treatment. This observation is also confirmed by significantly different Cl2p patterns for the untreated and the treated sensors (Figure 9(d)). The intensity of the Cl2p peak for the untreated sensor is significantly larger than the one for the treated sensor with a minimum chloride content (Figure 9(d))

Based on the XPS test results, AgCl must be the main silver compound that forms during anodization process of sensor preparation. Conditioning of the sensor in NaOH solution results in dechlorination of the AgCl layer and formation of silver oxide compounds (Ag_2O and AgO). This process subsequently shifts the sensor's OCP towards the cathodic values, for example, 100 mV versus SCE.

4. Conclusions

In this paper, the stability and reproducibility of OCP response of sensors with different thickness, morphology, and microstructure of the AgCl layer (sensors A and D) were monitored in alkaline solution. Based on the outcomes, the following conclusions can be drawn:

(i) The variation in the sensors' response in highly alkaline medium depends on the anodization regime used for the sensor's preparation and the chloride concentration in the medium. Sensor A (prepared at a low-current density of 0.5 mA/cm^2) was found to be more sensitive, reliable, and reproducible than sensor D (prepared at high-current density of 4 mA/cm^2).

(ii) The sensor's calibration curve in alkaline solution represents an excellent linear relationship ($R^2 = 0.999$) between the activity of chloride ions and the sensor's OCP at chloride concentration higher than 8 mM.

(iii) The results obtained in this work confirm the previously found alkalinity-dependent character of the chloride detection limit. In the pH range of concrete pore solution (12.6–13.6), the detection limit is 4 mM chloride content. Below this limit, the hydroxide ions interfere with the sensors' response.

(iv) In chloride-free medium, AgCl gradually transforms to silver oxides. The process is reversible, that is, the AgCl will gradually recover upon the addition (or in a subsequent presence) of chloride ions. The time needed for gradual transformation of silver oxides to AgCl and a stable Ag/AgCl response depends on the chloride concentration in the medium, impeded at lower chloride concentration (e.g., 125 mM) and relatively rapid at high chloride content (e.g., 1 M).

(v) The instability of an AgCl layer is a major drawback for the application of an Ag/AgCl electrode as chloride sensor in chloride-free alkaline medium. In this condition, the sensor's OCP shifts towards more anodic values. This is in line with the transformation of silver chloride to silver oxide. XPS analysis confirms that this instability is related to AgCl dechlorination and transformation of the Ag/AgCl interface to a more complex, Ag/AgCl/Ag_2O interface.

The experimental evidence in this paper indicates a well-defined feasibility for the application of Ag/AgCl electrodes as chloride sensors in alkaline medium, as concrete. In this regard, the chloride detection limit and reaction constraints at the sensor's surface for the sensitivity and reversibility of the sensors are taken into account.

Data Availability

The data used to support the findings of this study are available from the corresponding author upon request.

Conflicts of Interest

The authors declare no conflicts of interest.

References

[1] C. P. Atkins, J. D. Scantlebury, P. J. Nedwell, and S. P. Blatch, "Monitoring chloride concentrations in hardened cement pastes using ion selective electrodes," *Cement and Concrete Research*, vol. 26, no. 2, pp. 319–324, 1996.

[2] M. F. Montemor, J. H. Alves, A. M. Simoes et al., "Multiprobe chloride sensor for in situ monitoring of reinforced concrete structures," *Cement and Concrete Composites*, vol. 28, no. 3, pp. 233–236, 2006.

[3] U. M. Angst and R. Polder, "Spatial variability of chloride in concrete within homogeneously exposed areas," *Cement and Concrete Research*, vol. 56, pp. 40–51, 2014.

[4] M. A. Climent-Llorca, E. Viqueira-Perez, and M. M. Lopez-Atalaya, "Embeddable Ag/AgCl sensors for in-situ monitoring chloride contents in concrete," *Cement and Concrete Research*, vol. 26, no. 8, pp. 1157–1161, 1996.

[5] B. Elsener, L. Zimmermann, and H. Bohni, "Non-destructive determination of the free chloride content in cement-based materials," *Materials and Corrosion*, vol. 54, no. 6, pp. 440–446, 2003.

[6] Y. S. Femenias, U. Angst, F. Caruso, and B. Elsener, "Ag/AgCl ion-selective electrodes in neutral and alkaline environments containing interfering ions," *Materials and Structures*, vol. 49, no. 7, pp. 2637–2651, 2016.

[7] M. Jin, L. Jiang, M. Lu, and S. Bai, "Monitoring chloride ion penetration in concrete structure based on the conductivity of graphene/cement composite," *Construction and Building Materials*, vol. 136, pp. 394–404, 2017.

[8] D. Dobos, *Electrochemical Data: A Handbook for Electrochemists in Industry and Universities*, Elsevier Science and Technology, Amsterdam, Netherlands, 1975.

[9] G. Vera, A. Hidalgo, M. A. Climent, C. Andrade, and C. Alonso, "Chloride-ion activities in simplified synthetic concrete pore solutions: the effect of the accompanying ions," *Journal of the American Ceramic Society*, vol. 83, no. 3, pp. 640–644, 2000.

[10] A. Hidalgo, G. Vera, M. A. Climent, C. Andrade, and C. Alonso, "Measurements of chloride activity coefficients in real Portland cement paste pore solutions," *Journal of the American Ceramic Society*, vol. 84, no. 12, pp. 3008–3012, 2001.

[11] J. M. Gandia-Romero, R. Bataller, P. Monzón et al., "Characterization of embeddable potentiometric thick-film sensors for monitoring chloride penetration in concrete," *Sensors and Actuators B: Chemical*, vol. 222, pp. 407–418, 2016.

[12] M. Jin, J. Xu, L. Jiang, Y. Xu, and H. Chu, "Investigation on the performance characteristics of chloride selective electrode in concrete," *Ionics*, vol. 21, no. 10, pp. 2981–2992, 2015.

[13] M. A. Climent, C. Anton, G. de Vera, A. Hidalgo, and C. Andrade, "The interference of hydroxide ions in the potentiometric determination of free chloride in cement paste pore solution", in *Proceedings of the International RILEM Conference on Advances in Construction Materials Through Science and Engineering*, C. Leung and K. T. Wan, Eds., pp. 655–662, Hong Kong, China, September 2011.

[14] G. de Vera, M. A. Climent, C. Anton, A. Hidalgo, and C. Andrade, "Determination of the selectivity coefficient of a chloride ion selective electrode in alkaline media simulating the cement paste pore solution," *Journal of Electro Analytical Chemistry*, vol. 639, no. 1-2, pp. 43–49, 2010.

[15] M. R. Neuman, *Biopotential Electrodes, The Biomedical Engineering Handbook*, Chapter 8, CRC Press LLC, Boca Raton, FL, USA, 2000.

[16] X. J. Gao, J. Zhang, Y. Z. Yang, and S. Lu, "Preparation of chloride ion selective electrode and its potential response to different chloride solutions representing concrete environments," *Materials Science Forum*, vol. 675–677, pp. 537–541, 2011.

[17] X. Shi, Z. Ye, A. Muthumani, Y. Zhang, J. F. Dante, and H. Yu, "A corrosion monitoring system for existing reinforced concrete structures," Tech. Rep. No. FHWA-OR-RD-15–14, Federal Highway Administration, Washington, DC, USA, 2015.

[18] F. Pargar, D. A. Koleva, and K. van Breugel, "Determination of chloride content in cementitious materials: from fundamental aspects to application of Ag/AgCl chloride sensors," *Sensors*, vol. 17, no. 11, p. 2482, 2017.

[19] H. Lal, H. R. Thirsk, and W. F. K. Wynne-Jones, "A study of the behaviour of polarized electrodes. Part I. The silver/silver halide system," *Transactions of the Faraday Society*, vol. 47, pp. 70–77, 1951.

[20] T. Katan, H. Gu, and D. N. Bennion, "Analysis of porous electrodes with sparingly soluble reactants IV. Application to particulate bed electrode: Ag/AgCl system," *Journal Electrochemical Society*, vol. 123, no. 9, pp. 1370–1376, 1976.

[21] V. I. Birss and C. K. Smith, "The anodic behavior of silver in chloride solutions—I. The formation and reduction of thin silver chloride films," *Electrochimica Acta*, vol. 32, no. 2, pp. 259–268, 1987.

[22] P. Pargar, H. Kolev, D. A. Koleva, and K. van Breugel, "Microstructure, surface chemistry and altered response of Ag|AgCl sensors in alkaline media," *Journal of Materials Science*, vol. 53, no. 10, pp. 7527–7550, 2018.

[23] D. A. Shirley, "High-resolution X-ray photoemission spectrum of the valence bands of gold," *Physical Review B*, vol. 5, no. 12, pp. 4709–4714, 1972.

[24] B. J. Polk, A. Stelzenmuller, G. Mijares, W. MacCrehan, and M. Gaitan, "Ag/AgCl microelectrodes with improved stability for microfluidics," *Sensors and Actuators B: Chemical*, vol. 114, no. 1, pp. 239–247, 2006.

[25] F. Svegl, K. Kalcher, Y. J. Grosse-Eschedor, M. Balonis, and A. Bobrowski, "Detection of chlorides in pore water of cement-based materials by potentiometric sensors," *Journal of the Rare Metal Materials and Engineering*, vol. 35, no. 3, pp. 232–237, 2006.

[26] S. Karthick, S. J. Kwon, H. S. Lee, S. Muralidharan, V. Saraswathy, and R. Natarajan, "Fabrication and evaluation of a highly durable and reliable chloride monitoring sensor for civil infrastructure," *RSC Advances*, vol. 7, no. 50, pp. 31252–31263, 2017.

[27] G. S. Duffo, S. B. Farina, and C. M. Giordano, "Characterization of solid embeddable reference electrodes for corrosion monitoring in reinforced concrete structures," *Electrochimica Acta*, vol. 54, no. 3, pp. 1010–1020, 2009.

[28] U. Angst, B. Elsener, C. K. Larsen, and O. Vennesland, "Potentiometric determination of the chloride ion activity in cement-based materials," *Journal of Applied Electrochemistry*, vol. 40, no. 3, pp. 561–573, 2010.

[29] F. Pargar, D. A. Koleva, H. Kolev, and K. van Breugel, "The onset of chloride-induced corrosion in reinforced cement-based materials as verified by embeddable chloride sensors," in *Concrete Durability*, pp. 23–55, Springer International Publishing, Basel, Switzerland, 2017.

[30] W. J. McCarter and Ø. Vennesland, "Sensor systems for use in reinforced concrete structures," *Construction and Building Materials*, vol. 18, no. 6, pp. 351–358, 2004.

[31] S. Muralidharan, V. Saraswathy, A. Madhavamayandi, K. Thangavel, and N. Palaniswamy, "Evaluation of embeddable potential sensor for corrosion monitoring in concrete structures," *Electrochimica Acta*, vol. 53, no. 24, pp. 7248–7254, 2008.

[32] H. Suzuki and T. Taura, "Thin-film Ag/AgCl structure and operational modes to realize long-term storage," *Journal of the Electrochemical Society*, vol. 148, no. 12, pp. E468–E474, 2001.

[33] R. G. Du, R. G. Hu, R. S. Huang, and C. J. Lin, "In situ measurement of Cl^- concentrations and pH at the reinforcing steel/concrete interface by combination sensors," *Analytical Chemistry*, vol. 78, no. 9, pp. 3179–3185, 2006.

[34] U. Angst and O. Vennesland, "Detecting critical chloride content in concrete using embedded ion selective electrodes–effect of liquid junction and membrane potentials," *Materials and Corrosion*, vol. 60, no. 8, pp. 638–643, 2009.

[35] A. V. Naumkin, A. Kraut-Vass, S. W. Gaarenstroom, and C. J. Powell, *NIST X-Ray Photoelectron Spectroscopy Database*, NIST Standard Reference Database 20, Version 4.1. Nat'l Std. Ref. Data Series (NIST NSRDS), National Institute of Standards and Technology, Gaithersburg, MD, USA, 2012.

[36] V. K. Kaushik, "XPS core level spectra and Auger parameters for some silver compounds," *Journal of Electron Spectroscopy and Related Phenomena*, vol. 56, no. 3, pp. 273–277, 1991.

[37] F. Moulder, W. F. Sticke, P. E. Sobol, and K. D. Bombel, *Handbook of X-Ray Photoelectron Spectroscopy*, J. Castain, Ed., Physical Electron Division, Perkin-lmer Corporation, Eden Prairie, MN, USA, 2nd edition, 1992.

[38] A. M. Ferraria, A. P. Carapeto, and A. M. Botelho do Rego, "X-ray photoelectron spectroscopy: silver salts revisited," *Vacuum*, vol. 86, no. 12, pp. 1988–1991, 2012.